Received: 26 October 2017 | Revised: 25 March 2018 | Accepted: 30 March 2018

DOI: 10.1002/hbm.24079

RESEARCH ARTICLE

WILEY

Neuroplasticity and network connectivity of the motor cortex following stroke: A transcranial direct current stimulation study

Brenton Hordacre[1] | Bahar Moezzi[2] | Michael C. Ridding[2]

[1]The Sansom Institute for Health Research, School of Health Sciences, The University of South Australia, Adelaide 5001, Australia

[2]The Robinson Research Institute, Adelaide Medical School, The University of Adelaide, Adelaide 5005, Australia

Correspondence
Brenton Hordacre, The Sansom Institute for Health Research, School of Health Sciences, City East Campus, GPO Box 2471, Adelaide 5001, Australia.
Email: brenton.hordacre@unisa.edu.au

Funding information
National Health and Medical Research Council (NHMRC), Grant/Award Number: 1125054; Sylvia and Charles Viertel Charitable Foundation Clinical Investigator Award, Grant/Award Number: VTL2016CI009

Abstract

Transcranial direct current stimulation (tDCS) is a noninvasive brain stimulation technique that has potential for clinical utility in neurorehabilitation. However, recent evidence indicates that the responses to tDCS are highly variable. This study investigated whether electroencephalographic (EEG) measures of functional connectivity of the target network were associated with the response to ipsilesional anodal tDCS in stroke survivors. Ten chronic stroke patients attended two experimental sessions in a randomized cross-over trial and received anodal or sham tDCS. Single-pulse transcranial magnetic stimulation was used to quantify change in corticospinal excitability following tDCS. At the beginning of each session, functional connectivity was estimated using the debiased-weighted phase lag index from EEG recordings at rest. Magnetic resonance imaging identified lesion location and lesion volume. Partial least squares regression identified models of connectivity which maximally accounted for variance in anodal tDCS responses. Stronger connectivity of a network with a seed approximating the stimulated ipsilesional motor cortex, and clusters of electrodes approximating the ipsilesional parietal cortex and contralesional frontotemporal cortex in the alpha band (8–13 Hz) was strongly associated with a greater increase of corticospinal excitability following anodal tDCS. This association was not observed following sham stimulation. Addition of a structural measure(s) of injury (lesion volume) provided an improved model fit for connectivity between the seed electrode and ipsilesional parietal cortex, but not the contralesional frontotemporal cortex. TDCS has potential to greatly assist stroke rehabilitation and functional connectivity appears a robust and specific biomarker of response which may assist clinical translation of this therapy.

KEYWORDS

electroencephalography, magnetic resonance imaging, motor cortex, plasticity, stroke, transcranial direct current stimulation

1 | INTRODUCTION

Stroke is a leading cause of long-term disability in the adult population (Roger et al., 2012). The emergence of chronic diseases as a global health challenge (Murray et al., 2012; Yach, Hawkes, Gould, & Hofman, 2004) and an aging population (He, Goodkind, & Kowal, 2016) suggests that the incidence of stroke will continue to rise. In the acute post stroke period over two thirds of patients experience some level of reduced upper limb function, while 15%–30% of stroke survivors suffer permanent motor impairments despite extensive rehabilitation (Roger et al., 2011). Interventions capable of improving the efficiency or capacity for functional recovery are likely to be highly beneficial to stroke survivors, while also reducing financial and resource burden on health care systems.

Several noninvasive brain stimulation (NIBS) techniques have shown some promise in facilitating functional improvements and alleviating impairment after stroke. Following stroke ipsilesional corticospinal excitability is reduced, with subsequent increases in excitability associated with greater recovery of function (Swayne, Rothwell, Ward, & Greenwood, 2008; Traversa, Cicinelli, Pasqualetti, Filippi, & Rossini, 1998). Therefore, one approach is to apply NIBS to the lesioned motor cortex to increase corticospinal excitability. Several studies have reported behavioral improvements following stroke using this approach (Boggio et al., 2007; Hummel et al., 2005; Khedr, Ahmed, Fathy, &

TABLE 1 Participant demographics and clinical characteristics

Subject	Age	Sex	Handedness	Time since stroke (months)	Lesion location	Lesion volume (cm^3)	mRS
P01	76	M	R	19	Right temporal	2.8	1
P02	74	F	R	12	Left fronto-temporo-parietal	50.7	2
P03	43	M	L	17	Left insula, temporo-parietal	44.1	1
P04	46	M	R	21	Right basal ganglia	4.1	1
P05	74	M	R	13	Left posterior-frontal	44.9	2
P06	58	M	R	16	Right fronto-temporal	5.8	1
P07	76	F	R	17	Right basal ganglia	2.7	2
P08	90	F	R	16	Right temporo-parietal	20.6	2
P09	34	M	R	15	Right centrum semiovale and posterior limb of internal capsule	4.5	2
P10	67	M	R	13	Right parietal-occipital	4.9	1

Note. Abbreviation: mRS, modified ranking scale (range 0–6).

Rothwell, 2005; Talelli, Greenwood, & Rothwell, 2007), suggesting NIBS has potential to be employed for therapeutic purposes and facilitate stroke recovery.

However, the expectation that behavioral and physiological responses to NIBS are largely homogeneous and predictable does not appear to be true with evidence indicating high intersubject variability. Several recent studies with healthy participants have highlighted responses following NIBS are variable (Hamada, Murase, Hasan, Balaratnam, & Rothwell, 2013; Hordacre et al., 2017a; López-Alonso, Cheeran, Río-Rodríguez, & Fernández-del-Olmo, 2014; Müller-Dahlhaus, Orekhov, Liu, & Ziemann, 2008). Furthermore, Cochrane reviews have been unable to support use of NIBS as an intervention for stroke survivors as a result of highly variable responses (Elsner, Kugler, Pohl, & Mehrholz, 2016; Hao, Wang, Zeng, & Liu, 2013). Although producing the desired functional benefit in some stroke survivors, NIBS may not be a one-size-fits-all intervention and it may be that some patients experience no functional benefit from cortical stimulation (Hesse et al., 2011; Rossi, Sallustio, Di Legge, Stanzione, & Koch, 2013). Biomarkers to identify those likely to respond strongly to stimulation are required to improve clinical translation.

Multiple factors have been identified as characteristics which partly shape NIBS responses. Briefly, these factors include age, attention, genetics, history of physical activity, and characteristics of the interneuron network activated by stimulation (Hamada et al., 2013; Ridding & Ziemann, 2010). Recently, we also demonstrated in healthy adults that stronger connectivity of the stimulated sensorimotor network in the high beta frequency (20–30Hz) was associated with a greater increase in corticospinal excitability following a facilitatory NIBS protocol, namely, anodal transcranial direct current stimulation (tDCS) (Hordacre et al., 2017b). It may be that differences in connectivity of the target network in these healthy participants reflected, at least in part, some of the previously identified characteristics associated with response to NIBS (Hamada et al., 2013; Ridding & Ziemann, 2010). In stroke patients, additional variability may be introduced through heterogeneous characteristics of lesion location, lesion size, time since stroke, medications, and post stroke treatments (Adeyemo, Simis, Macea, & Fregni, 2012). Therefore, understanding how the residual network influences and modulates response to NIBS is an important question which may have potential to assist appropriate patient selection and facilitate better clinical translation. The purpose of this study was to investigate whether EEG measures of functional connectivity of the target network were associated with the response to ipsilesional anodal tDCS in stroke survivors. A secondary aim was to determine whether additional clinical characteristics and a structural measure of injury could provide an improved model to account for variance in tDCS response. Based on our previous work in healthy adults (Hordacre et al., 2017b), we hypothesized that stroke survivors with greater ipsilesional sensorimotor network connectivity would have a greater facilitation of corticospinal excitability following anodal tDCS.

2 | MATERIALS AND METHODS

2.1 | Participants

Ten chronic stroke patients (7 male, aged 63.8 (SD 17.9) years) were tested. Inclusion criteria for this study were $\geq$12 month post first ever ischaemic stroke with motor impairment and not currently undertaking an inpatient or outpatient rehabilitation program. Exclusion criteria were prestroke disability, inability to verbally communicate and provide informed consent, and any contraindication to transcranial magnetic stimulation (TMS) or tDCS, including metallic implants, pregnancy, a history of seizures and medications known to alter central nervous system excitability (Rossi, Hallett, Rossini, & Pascual-Leone, 2011). Demographics and clinical characteristics of participants are reported in Table 1. Participants provided written informed consent in accordance with the World Medical Association Declaration of Helsinki. Ethical approval

to conduct the study was provided by the institutional ethics committee (University of Adelaide Human Research Ethics Committee).

2.2 | Experimental protocol

This was a participant blind randomized cross-over trial. On admission to the study, participants were randomized to initially receive either anodal or sham tDCS to the lesioned primary motor cortex (M1). Participants returned for a second experimental session to receive the alternative form of stimulation. The order of the experimental sessions was counterbalanced and separated by at least 7 days (mean 25.0 (*SD* 14.0) days) to avoid carry over effects of the initial stimulation protocol. The modified Rankin Scale (mRS) was used to quantify stroke disability on admission to the study. The mRS is a widely used, valid and reliable assessment of global disability scored on a 7 point scale ranging from 0 (no disability symptoms) to 6 (dead) (Banks & Marotta, 2007).

2.3 | Magnetic resonance imaging

Stroke diagnosis was confirmed using magnetic resonance imaging (MRI) acquired on a Siemens Trio 3 T scanner (Siemens, Erlangen, Germany). The protocol contained a high-resolution T1-weighted images (TR = 8.6 ms, TE = 4 ms, slice thickness = 7 mm), fluid-attenuated inversion-recovery (FLAIR; TR = 9,000 ms, TE = 93 ms, slice thickness = 4.5 mm), proton density-weighted and T2-weighted brain images (TR = 3,890 ms, TE = 15 ms, slice thickness = 4.5 mm). Lesion location was identified by an experienced radiologist and lesion volume was outlined by hand and analyzed using MRIcron (www.mccauslandcenter.sc.edu/crnl/mricron/) similar to previous studies (Dubovik et al., 2012; Quinlan et al., 2015).

2.4 | EEG acquisition

At the beginning of each session, 3 min of EEG was acquired using an ASA-lab EEG system (ANT Neuro, Enschede, Netherlands) with 64 sintered Ag-AgCl electrodes in standard 10-10 positions. During data collection, participants were seated in a comfortable chair and asked to relax while refraining from speaking or moving, keep their eyes open and maintaining their gaze toward a fixation point straight ahead. Participants were also asked to not actively engage in any cognitive or mental tasks during the data collection period. Signals were sampled at 2,048 Hz, amplified 20×, filtered (high pass, DC; low pass 553 Hz) and referenced to the average of all electrodes. Impedance was kept below 5 kΩ and recorded data were stored on a computer for offline analysis.

2.5 | Electromyography

Surface electromyography (EMG) was used to record motor evoked potentials (MEPs) evoked by single pulse TMS. MEPs were recorded from the first dorsal interosseous (FDI) muscle of the paretic hand using a belly-tendon electrode montage using Ag-AgCl surface electrodes (Ambu, Ballerup, Denmark). Initially, the skin overlying the FDI of the paretic hand was prepared by cleaning with alcohol and lightly abrading with NuPrep paste. A ground strap placed around the wrist of the paretic arm. Signals were sampled at 5 kHz (CED 1401; Cambridge Electronic Design, Cambridge, UK), amplified (1,000×) (CED 1902; Cambridge Electronic Design or Digitimer D360, Welwyn Garden City, Herts, UK), filtered (20–1000 Hz) and stored for offline analysis (Signal v4.09, Cambridge Electronic Design, Cambridge, UK).

2.6 | Transcranial magnetic stimulation

Single pulse TMS was used to quantify corticospinal excitability at baseline and at multiple time points following anodal tDCS. TMS was applied with a monophasic waveform via a figure-of-eight magnetic coil (external wing diameter 90mm) connected to a Magstim 200 magnetic stimulator (Magstim, Whitland, Dyfed, UK). Stimulation was applied to the lesioned M1 hand representation, with the coil held tangentially to the scalp and handle pointing 45° posterolaterally to induce a posterior–anterior current. The optimal coil position for evoking a MEP in the paretic FDI muscle at rest was located and marked on the scalp using a water-soluble felt tip marker. Rest motor threshold (RMT) was defined as the minimum stimulus intensity required to evoke an MEP with peak-to-peak amplitude $\geq$50 μV in at least five out of ten consecutive trials in the relaxed FDI. Corticospinal excitability was quantified by evoking MEPs at 120% RMT and measuring peak-peak amplitudes. Baseline corticospinal excitability was assessed by averaging two blocks of 20 MEPs, separated by a short rest interval, to provide a reliable estimate of MEP amplitude (Goldsworthy, Hordacre, & Ridding, 2016). Following tDCS, blocks of 20 MEPs were recorded at 5, 10, 20, and 30 min following stimulation. TMS pulses were delivered with an interstimulus interval of 5 s ± 10%. Trials were visually inspected at high gain in a 200 ms window prior to the TMS pulse for prestimulus EMG. Those contaminated with background EMG were removed (average of 0.5 (*SD* 0.9) trials removed per block).

2.7 | Transcranial direct current stimulation

Anodal tDCS was applied using a NeuroConn DC Stimulator Plus (NeuroConn, Ilmenau, Germany). The anode was positioned over the previously marked lesioned M1 hot spot and the cathode over the contralateral orbit using saline-soaked surface sponge electrodes (35 cm^2). Real stimulation was delivered at an intensity of 1 mA for 20 min including a 30 s ramp up to 1 mA at the start and a 30 s ramp down to 0 mA at the end. For sham stimulation, the current was initially ramped up for the first 30 s to mimic the initial sensation perceived with tDCS and then ramped down for 30 s (see Figure 1 for electrode montage and stimulation settings). This is an effective method of delivering sham tDCS (Gandiga, Hummel, & Cohen, 2006). During stimulation, participants were asked to relax their hand while their upper limb was supported in a comfortable position.

2.8 | EEG preprocessing and analysis

EEG data were exported to MATLAB 9.2.0 (MathWorks, Inc., Natick, MA) for pre-processing and analysis. Data were filtered using a second order Butterworth filter with a bandpass from 1 to 80 Hz and also a band stop filter 48–52 Hz. Bad channels were then removed and EEG

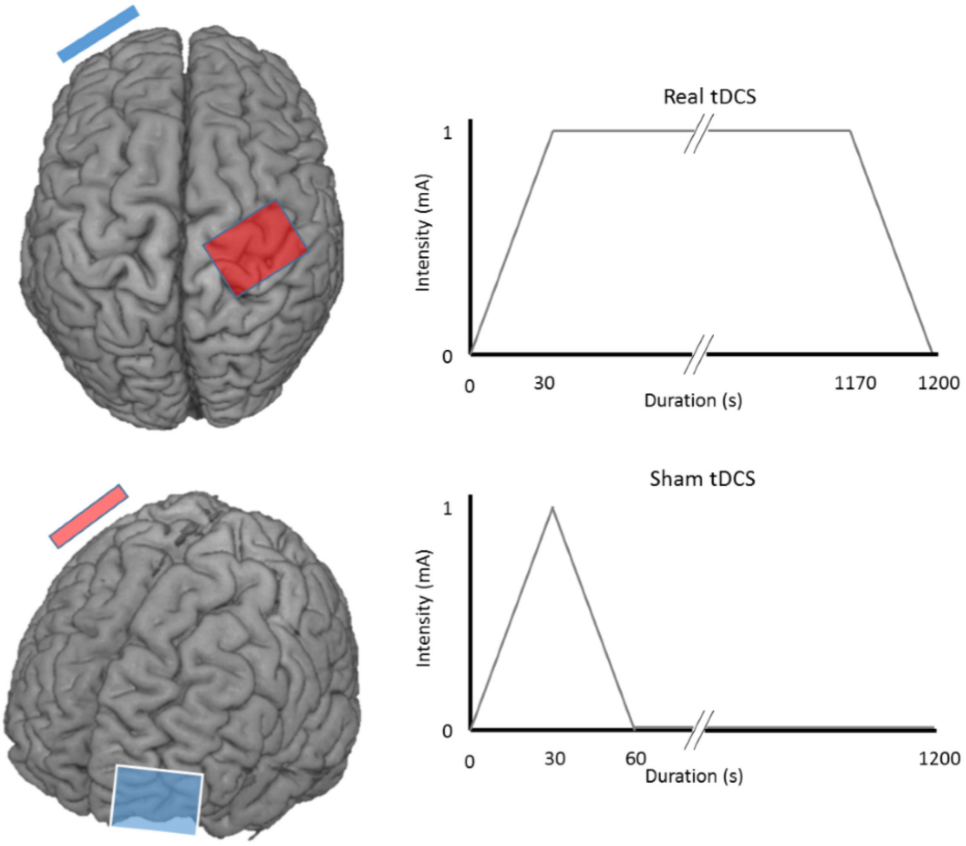

FIGURE 1 Stimulation protocol. tDCS electrodes are positioned over the lesioned M1 (right hemisphere in this example) and contralateral orbit. Anode is red, cathode is blue. Real tDCS is delivered for 20 min at 1 mA including a 30 s ramp up to 1 mA at the start and a 30 s ramp down at the end. Sham tDCS mimics the sensation of tDCS by beginning with a 30 s ramp up to 1 mA, then ramping down to 0 mA with no further current delivered to the cortex while the participant remained seated with electrodes in position until completion of the 20 min session (Gandiga et al., 2006) [Color figure can be viewed at wileyonlinelibrary.com]

data was segmented into 180 one-second epochs and visually inspected (no epochs removed). Data was then submitted to an independent component analyses using the EEGLAB fast ICA function (Delorme & Makeig, 2004) to identify and remove nonphysiological artefactual components (e.g., eye blinks, scalp muscle activity). Following artefact removal, missing channels were interpolated. For patients who had a left M1 lesions, data were flipped about the sagittal plane for subsequent analysis.

The debiased weighted phase lag index (dwPLI) was computed to estimate functional connectivity between electrodes (Vinck, Oostenveld, Van Wingerden, Battaglia, & Pennartz, 2011) using the FieldTrip toolbox in MATLAB (Oostenveld, Fries, Maris, & Schoffelen, 2011). The dwPLI is a conservative analytical method to estimate connectivity based on phase consistency and weighting against zero phase lag relationships (Vinck et al., 2011). This approach limits the effects of volume conduction and common reference problems (Bastos & Schoffelen, 2016). The dwPLI values range from 0 (negative values can incidentally occur due to limited sampling) and 1 (maximum phase coupling). Connectivity values were calculated between a seed electrode approximating the lesioned right M1 (C4) and all other electrodes. The dwPLI was determined for delta (1–3 Hz), theta (4–7 Hz), alpha (8–13 Hz), low beta (14–19 Hz), high beta (20–30 Hz), and gamma (31–45 Hz) spectral frequencies.

2.9 | Partial least squares analysis

Partial least squares (PLS) regression was used to identify a model of connectivity between the seed electrode (C4) and all other electrodes to maximally predict variance in the response to anodal tDCS. PLS regression modelling was performed using the N-way Toolbox for MATLAB (Andersson & Bro, 2000). The dependent variable was the response to anodal tDCS, calculated as the average amplitude of post tDCS MEP blocks normalized to baseline, and the independent variables were dwPLI between C4 and all other electrodes. Separate PLS regression analyses were performed for the different frequency bands. PLS modeling has several advantages, including ability to handle a greater number of independent variables than observations without increased risk of Type I error, and the capacity to handle nonorthogonal independent variables (Cramer, 1993). Similar to previous studies, a threshold relative to the absolute value of the maximal correlation coefficient is required for correlation coefficients to include in the PLS model (Hordacre et al., 2017b; Menzies et al., 2007). There is a negative relationship between threshold and proportion of variance predicted by PLS modeling. To objectively select a threshold appropriate for this dataset, we plotted the R^2 value for all frequency bands with thresholds ranging from 0 to 1, increasing in steps of 0.01 (Figure 2).

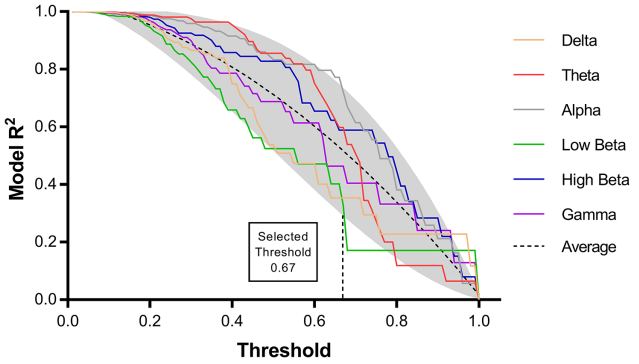

FIGURE 2 The fitted model R^2 for each frequency band decreases with increasing threshold for the correlation coefficients included in the PLS model. Threshold was selected based on the point at which a model R^2 continuously (>3 data points) fell below a cutoff line representing the 90th percentile (shaded grey area) of the average for all frequency bands (black dash line) [Color figure can be viewed at wileyonlinelibrary.com]

The threshold was selected based on the point which the model R^2 value for any frequency fell below a 90th percentile cutoff for more than 3 consecutive data points indicating that the model fit was dramatically reduced as a result of the increased threshold. The threshold selected was 0.67 which is more conservative than used previously (Hordacre et al., 2017b). The first component was used for all PLS models generated. As a pre-processing step, data were mean centered and submitted to a direct orthogonal signal correction (Westerhuis, de Jong, & Smilde, 2001). These steps remove the largest independent measures orthogonal to the tDCS plasticity response, resulting in a more efficient PLS model using fewer components. Fitted PLS models were cross-validated using a leave-one-out and predict procedure, where data from one subject was iteratively removed, to determine their predictive values. The cross-validated R^2 quantifies the prediction accuracy determined by the ratio of prediction error to total variance in the actual data. Once PLS models were generated, clusters of electrodes, defined as having at least 3 adjacent electrodes in space with correlation coefficients above threshold, were identified in each PLS model. The mean dwPLI values of the identified clusters were then determined and correlated against the dependent variable (anodal or sham tDCS response). To determine that the identified PLS models were robust, a range of model thresholds were identified for which the identified electrode clusters remained.

2.10 | Statistical analysis

Statistical analyses were performed using SPSS software (IBM Corp., Released 2016, IBM SPSS Statistics for Windows, Version 24.0, Armonk, NY, USA) and MATLAB 9.2.0 (MathWorks, Inc., Natick, MA) with significance level set at $p < .05$. Normality of the data were checked, and where required, nonparametric statistics applied. RMT and baseline MEP amplitudes were compared between tDCS sessions using paired *t* tests. Plasticity responses to tDCS were analyzed using a 2 condition (anodal, sham) × 5 time (baseline, post 5 min, post 10 min, post 20 min, post 30 min) repeated measures ANOVA. Demographics, clinical, and neurophysiological characteristics were analyzed to determine their association with tDCS response using an independent *t* test (gender) and Pearson correlations (age, time since stroke, lesion volume, RMT, and baseline MEP amplitude). Average dwPLI across electrode clusters identified with PLS modeling were further analyzed with Pearson correlations or Spearman's rank correlations to determine the association with anodal and sham tDCS response, and corrected for multiple comparisons (Bonferroni correction). Regression models comprising functional connectivity, structural impairment, and clinical characteristics were compared using Bayesian information criteria (BIC) (Kass & Raftery, 1995). BIC determines the most appropriate regression model with lower values indicating a more efficient and/or better fit (a model difference <2 is negligible, 2–6 a small positive improvement, 6–10 a strong positive improvement, and >10 very strong positive improvement; Kass & Raftery, 1995). Finally, demographics, clinical, and neurophysiological characteristics were analyzed to determine their association with connectivity using an independent *t* test (gender) and Pearson correlations (age, time since stroke, lesion volume, RMT, and baseline MEP amplitude).

3 | RESULTS

Anodal tDCS was well tolerated by all participants without any side effects. One subject was unable to return for the second experiment (sham condition) as a result of medical complications unrelated to the study protocol. Data from this subject was not included when analyzing the effect of tDCS on corticospinal excitability, but was included to maximize statistical power when addressing the main research questions which was to determine whether baseline measures of connectivity were associated with response to anodal tDCS.

3.1 | Anodal tDCS did not increase corticospinal excitability

For the nine subjects who completed both anodal and sham tDCS sessions there were no significant differences in RMT (anodal 54.3% maximal stimulator output (MSO) (*SD* 8.4); sham 54.1% MSO (*SD* 9.5); $t_{(8)} = 0.16$, $p = .89$) or baseline MEP amplitude (anodal 0.88 mV (*SD* 1.0); sham 0.89 mV (*SD* 1.1); $t_{(8)} = 0.02$, $p = .98$) between sessions. Response to anodal tDCS was variable between participants which resulted in no main effect of condition ($F_{(1,8)} = 0.86$, $p = .38$), time ($F_{(2.5,20.1)} = 2.63$, $p = .09$), or condition × time interaction ($F_{(4,32)} = 0.26$, $p = .90$) indicating tDCS did not significantly change corticospinal excitability at the group level (see Figure 3 for response variability to tDCS). The grand average tDCS response for both anodal and sham stimulation was determined for all participants. The grand average tDCS response was calculated as the mean MEP amplitude post tDCS normalized to the mean baseline MEP amplitude. On average, post-tDCS MEP amplitudes were 95.9% (*SD* 39.5) of baseline following anodal stimulation and 96.6% (*SD* 38.1) of baseline following sham.

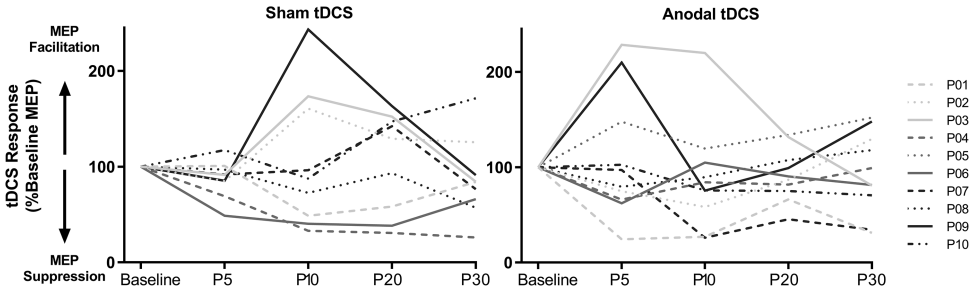

FIGURE 3 Individual change in corticospinal excitability following tDCS was variable across participants for both sham (left) and anodal (right) tDCS

3.2 | Clinical characteristics and demographics are not associated with anodal tDCS response

We further investigated participant demographics, clinical characteristics and baseline neurophysiological characteristics to determine if there was any correlation with response to anodal tDCS. Lesion volume ($r = .53$, $p = .12$), age ($r = -.50$, $p = .15$), gender ($t_{(8)} = 0.88$, $p = .41$), time since stroke ($r = -.35$, $p = .33$), RMT ($r = -.10$, $p = .77$), and baseline MEP amplitude ($r = -.17$, $p = .64$) were not associated with anodal tDCS response.

3.3 | EEG connectivity and tDCS response

PLS regression analyses were used to identify models of connectivity between a seed electrode approximating the lesioned M1 and the whole scalp that maximally predicted grand average anodal tDCS response. Models were generated for delta, theta, alpha, low beta, high beta, and gamma frequencies with the strongest relationship observed in alpha frequency (fitted PLS model $R^2 = 0.72$), which also had a high predictive value (cross validated $R^2 = 0.58$; Table 2).

The alpha PLS model identified two clusters of electrodes which predicted response to anodal tDCS. These clusters approximated the contralesional frontotemporal region and the ipsilesional parietal cortex (Figure 4) and remained present across a range of thresholds used to generate the alpha PLS model (threshold range 0.49–0.75) suggesting that the model of connectivity for predicting anodal tDCS response was robust. Connectivity between the lesioned M1 and each cluster was individually associated with response to anodal tDCS with stronger connectivity indicative of an increase in corticospinal excitability following stimulation (contralesional frontotemporal cluster, $r = .83$, $p = .02$ Bonferroni-corrected; ipsilesional parietal cluster, $r = .85$, $p = .01$ Bonferroni-corrected; Figure 4). Connectivity between the lesioned M1 and each cluster was not associated with sham tDCS response (contralesional frontotemporal cluster, $r = .25$, $p = .52$; ipsilesional parietal cluster, $r = 0.46$, $p = .22$).

The theta PLS model ($R^2 = 0.60$, cross-validated $R^2 = 0.40$) identified two clusters of electrodes which predicted response to anodal tDCS. The two clusters approximated the contralesional frontal cortex and the ipsilesional parietal-occipital cortex (Figure 5) and remained present across a range of thresholds used to generate the theta PLS model (threshold range 0.58–0.73) suggesting that the model of connectivity for predicting anodal tDCS response was robust. Connectivity with the ipsilesional parietal-occipital cortex was associated with response to anodal tDCS, but became insignificant following correction for multiple comparisons ($r = .71$, $p = .15$ Bonferroni-corrected; Figure 5). Connectivity with the contralesional frontal cortex was not associated with the anodal tDCS response (rho = 0.49, $p = 1.00$ Bonferroni-corrected). Sham tDCS response was not associated with the ipsilateral ($r = .30$, $p = .44$) or contralateral (rho = −0.17, $p = .67$) cluster.

The high beta PLS model ($R^2 = 0.59$, cross validated $R^2 = 0.56$) identified three clusters of electrodes which predicted response to anodal tDCS. The clusters approximated the contralesional frontal cortex, ipsilesional, frontal cortex and the ipsilesional parietal cortex (Figure 6) and remained present across a range of thresholds used to generate the high beta PLS model (threshold range 0.38–0.74) suggesting that the model of connectivity for predicting anodal tDCS response was robust. Connectivity with the ipsilesional frontal cortex was associated with response to anodal tDCS, but this association was insignificant following correction for multiple comparisons ($r = .74$, $p = .10$ Bonferroni-corrected; Figure 6). Connectivity with the contralesional frontal cortex (rho = 0.26, $p = 1.00$ Bonferroni-corrected) and ipsilesional parietal cortex (rho = 0.59, $p = .52$ Bonferroni-corrected) were not associated with the anodal tDCS response. Connectivity with the ipsilesional frontal cortex ($r = .31$, $p = .42$), ipsilesional parietal cortex (rho = 0.28, $p = .46$) and contralesional frontal cortex (rho = 0.42, $p = .27$) were not associated with the sham tDCS response.

PLS models for delta, low beta and gamma frequencies explained a lower proportion of variance in anodal tDCS response. The one cluster identified in the gamma PLS model (contralesional central cluster) was not associated with anodal (rho = 0.42, $p = 1.00$ Bonferroni-corrected)

TABLE 2 PLS models generated for anodal tDCS response and connectivity (dwPLI) in delta, theta, alpha, low beta, high beta, and gamma frequency bands

Frequency	Fitted R^2	Cross-validated R^2
Delta	0.35	0.35
Theta	0.60	0.40
Alpha	0.72	0.58
Low beta	0.33	0.16
High beta	0.59	0.56
Gamma	0.46	0.37

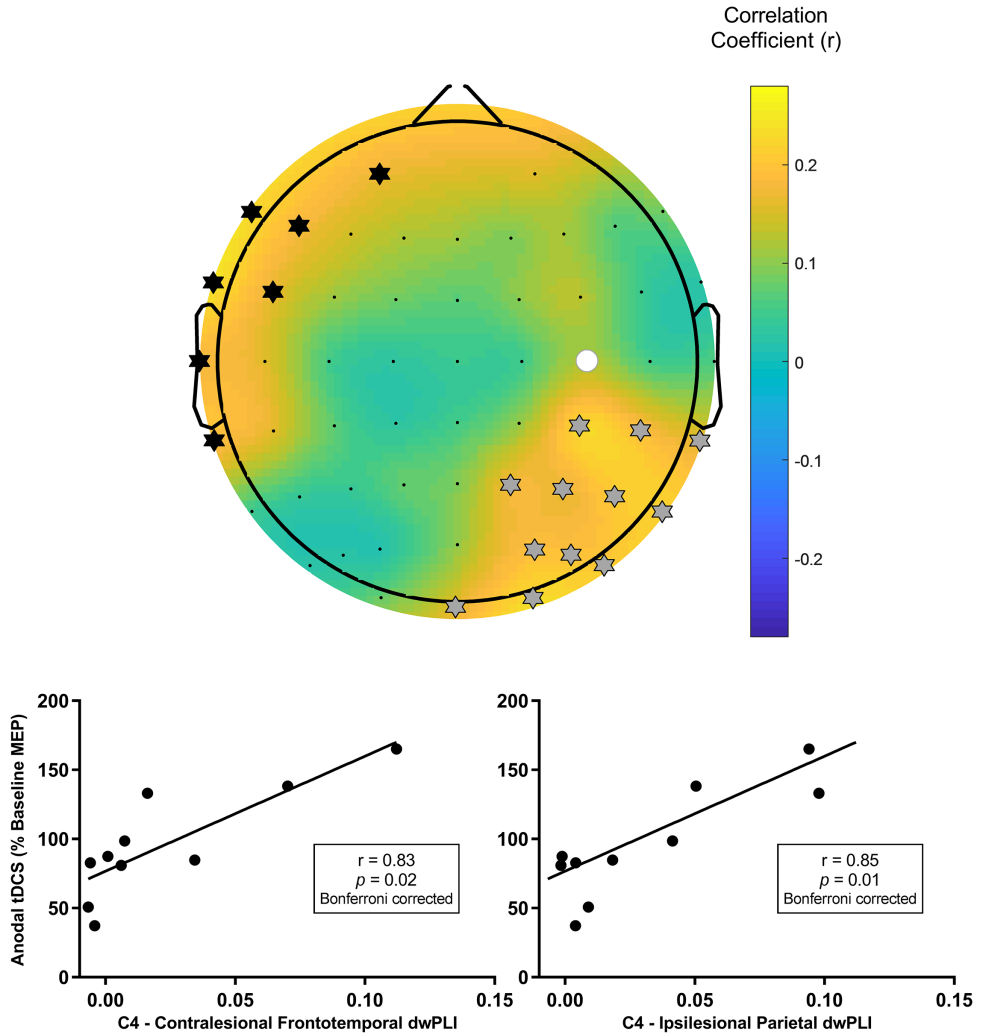

FIGURE 4 Connectivity between C4, approximating the target lesioned M1, and two clusters of electrodes approximating the contralesional frontotemporal cortex and ipsilesional parietal cortex in the alpha frequency band predicted response to anodal tDCS. (Top) A topographic plot of correlation coefficients from the PLS model correlating seed connectivity across whole scalp and tDCS response in alpha band. The seed electrode is shown with a filled white circle. Electrodes identified as being in a cluster approximating the contralesional frontotemporal cortex are marked with black stars. Electrodes identified as being in a cluster approximating the ipsilesional parietal cortex are marked with grey stars. Mean alpha band connectivity between C4 and the contralesional frontotemporal cortex (bottom left), and between C4 and the ipsilesional parietal cortex (bottom right), were individually associated with anodal tDCS response following correction for multiple comparisons [Color figure can be viewed at wileyonlinelibrary.com]

or sham tDCS response (rho = 0.35, $p = .36$). No electrodes clusters were identified in PLS models for delta or low beta frequencies.

3.4 | A model combining functional connectivity, lesion volume, and clinical characteristics to account for variance in anodal tDCS response

Regression models were generated for the two alpha band electrode clusters that were significantly associated with anodal tDCS response. A regression model (model 1) with dependent variable of anodal tDCS response and independent variable of dwPLI between the stimulated ipsilesional M1 and a cluster of electrodes approximating the ipsilesional parietal cortex in alpha frequency was significant ($R^2 = 0.72$, $p = .002$). Subsequent addition of independent variables resulted in lower BIC values indicating improvement over a model comprising functional connectivity only (model 1) to describe variance in anodal tDCS response (Table 3). However these improvements were not considered strong (Kass & Raftery, 1995) and should be viewed cautiously.

Similar regression models developed for dwPLI between the stimulated ipsilesional M1 and a cluster of electrodes approximating the contralesional frontotemporal cortex in alpha frequency did not improve on model 1 with BIC values increasing following addition of independent variables (Table 3). This suggests that regression model comprising functional connectivity provides the best fit to describe variance in anodal tDCS response.

3.5 | Clinical characteristics and demographics are not associated with connectivity

To further explore connectivity between the seed electrode and the two alpha band electrode clusters identified by PLS modelling we

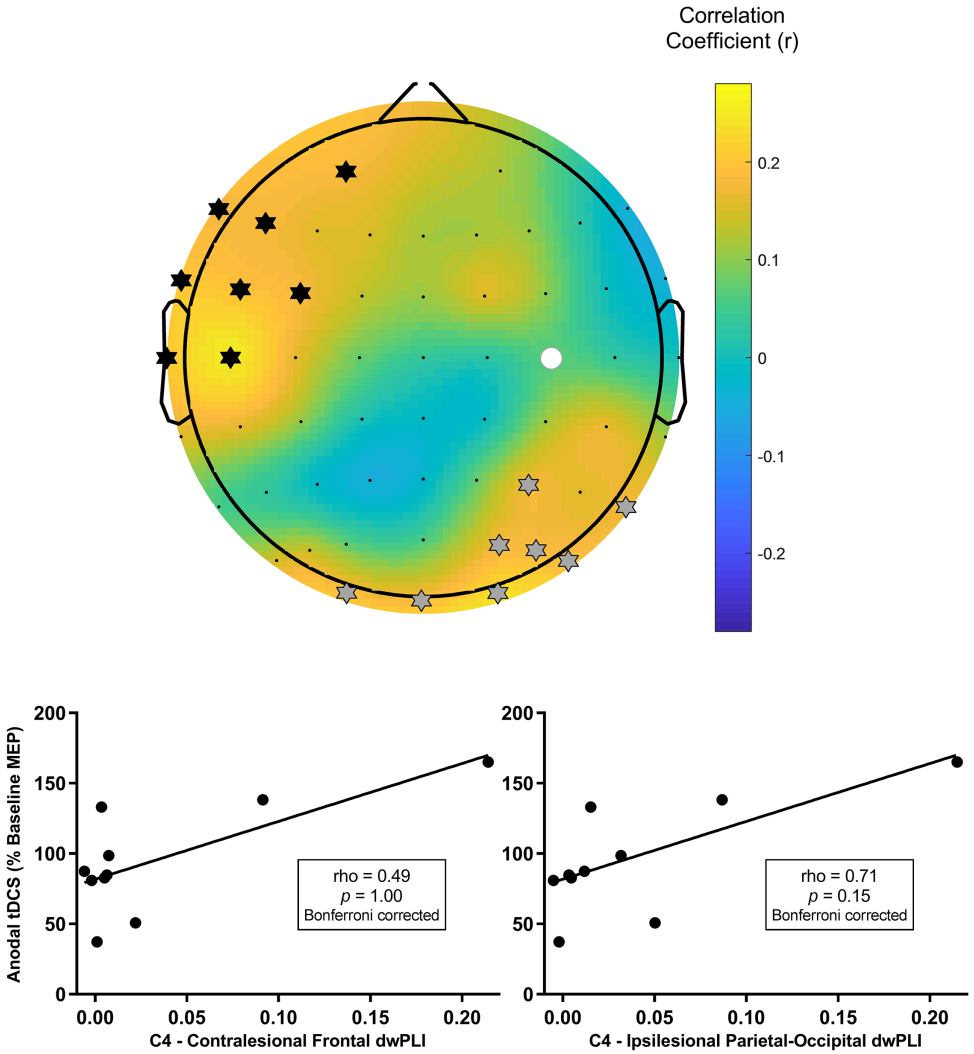

FIGURE 5 Connectivity between C4, approximating the target lesioned M1, and two clusters of electrodes approximating the contralesional frontal cortex and ipsilesional parietal-occipital cortex in the theta frequency band predicted response to anodal tDCS. (Top) A topographic plot of correlation coefficients from the PLS model correlating seed connectivity across whole scalp and tDCS response in theta band. The seed electrode is shown with a filled white circle. Electrodes identified as being in a cluster approximating the contralesional frontal cortex are marked with black stars. Electrodes identified as being in a cluster approximating the ipsilesional parietal-occipital cortex are marked with grey stars. (Bottom) Mean theta band connectivity between C4 and each cluster were not significantly associated with anodal tDCS response following correction for multiple comparisons [Color figure can be viewed at wileyonlinelibrary.com]

investigated associations with clinical characteristics, demographics and baseline neurophysiological characteristics. Connectivity between the seed electrode and ipsilesional parietal cluster was not associated with lesion volume ($r = .28$, $p = .44$), age ($r = -.54$, $p = .11$), gender ($t_{(8)} = 0.81$, $p = .44$), time since stroke ($r = -.08$, $p = .84$), RMT ($r = .15$, $p = .68$), and baseline MEP amplitude ($r = -.15$, $p = .69$). Similarly, connectivity between the seed electrode and contralesional frontotemporal cluster was not associated with lesion volume ($r = .59$, $p = .08$), age ($r = -.33$, $p = .35$), gender ($t_{(8)} = 1.22$, $p = .26$), time since stroke ($r = -.16$, $p = .65$), RMT ($r = -.01$, $p = .98$), and baseline MEP amplitude ($r = -.27$, $p = .45$).

4 | DISCUSSION

This study investigated whether response to anodal tDCS was associated with network connectivity when using a seed electrode approximating the target ipsilesional M1 in chronic stroke survivors. As expected, we observed large intersubject variability in response to anodal tDCS. Only 30% of participants responded with the anticipated increase in corticospinal excitability and we did not observe a group difference in the response to anodal or sham tDCS stimulation. Previous studies have also reported high intersubject variability for behavioral outcomes following tDCS in people with stroke (Hesse et al., 2011; Rossi et al., 2013; Tedesco Triccas et al., 2015), which limits the opportunity for this intervention to be used in a therapeutic manner. However, we were able to demonstrate that properties of the target brain network provided a strong and robust association with anodal tDCS responses. Specifically, a model of alpha band connectivity between a seed electrode approximating the stimulated ipsilesional M1 and clusters of electrodes approximating the ipsilesional parietal cortex and contralesional frontotemporal cortex was strongly associated with

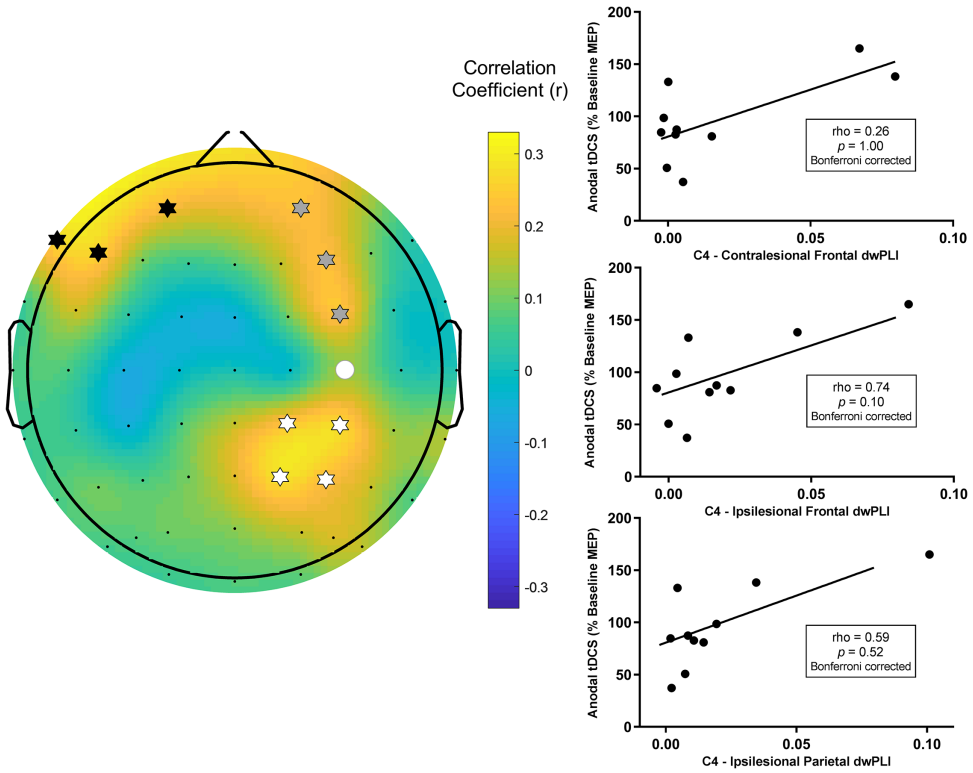

FIGURE 6 Connectivity between C4, approximating the target lesioned M1, and three clusters of electrodes approximating the contralesional frontal cortex, ipsilesional frontal cortex, and ipsilesional parietal cortex in the high beta frequency band predicted response to anodal tDCS. (Left) A topographic plot of correlation coefficients from the PLS model correlating seed connectivity across whole scalp and tDCS response in high beta band. The seed electrode is shown with a filled white circle. Electrodes identified as being in a cluster approximating the contralesional frontal cortex are marked with black stars. Electrodes identified as being in a cluster approximating the ipsilesional frontal cortex are marked with grey stars. Electrodes identified as being in a cluster approximating the ipsilesional parietal cortex are marked with white stars. (Right) Mean high beta band connectivity between C4 and each cluster were not significantly associated with anodal tDCS response following correction for multiple comparisons [Color figure can be viewed at wileyonlinelibrary.com]

modulation of corticospinal excitability following anodal tDCS ($R^2 = .72$). Stronger connectivity between M1 and each cluster of electrodes was individually associated with greater increases in corticospinal excitability. Similar relationships were not observed for sham tDCS suggesting this result is specific for anodal stimulation. The addition of lesion volume with connectivity between the seed electrode and ipsilesional parietal cluster provided a small positive improvement in accounting for variance in anodal tDCS response. However, the addition of lesion volume and clinical characteristics for the regression model with connectivity between the seed electrode and contralesional frontotemporal cluster provided no improvement in model fit. Knowing the properties of the target network may assist prediction of response to tDCS.

Behavioral evidence provides good support for our observation that network connectivity may influence neuroplastic responses. Following stroke, functional magnetic resonance imaging (fMRI) has been

TABLE 3 Regression models generated to account for variance in anodal tDCS response

	Ipsilesional parietal cluster				Contralesional frontotemporal cluster			
	R^2	*p*	BIC	ΔBIC	R^2	*p*	BIC	Δ BIC
Model 1	0.722	0.002	64.277	-	0.681	0.003	65.661	-
Model 2	0.863	0.001	59.514	4.763	0.695	0.016	67.501	−1.840
Model 3	0.866	0.005	61.606	2.671	0.711	0.047	69.266	−3.605
Model 4	0.904	0.009	60.561	3.713	0.823	0.040	66.671	−1.01

Model 1 included independent variable of functional connectivity (dwPLI) between the target ipsilesional M1 stimulated with anodal tDCS and the identified electrode cluster. Model 2 included independent variables of functional connectivity and lesion volume. Model 3 included independent variables of functional connectivity, lesion volume, and time since stroke. Model 4 included independent variables of functional connectivity, lesion volume, time since stroke, and age. The Bayesian information criteria (BIC) was used to select the most appropriate model. Lower BIC values indicate a more efficient and/or better fit model. ΔBIC represents change in BIC values from model 1.

used to demonstrate greater functional connectivity of the lesioned motor network is associated with a better recovery of motor function (Park et al., 2011; Quinlan et al., 2015). Similarly, in healthy adults, EEG markers of functional connectivity at baseline demonstrated strong predictive capacity for improvements on a motor learning task (Wu, Srinivasan, Kaur, & Cramer, 2014). While speculative, it may be that connectivity of brain networks involved in learning can affect efficiency and capability to acquire motor skills as a result of greater physiological capacity to explore and learn optimal strategies to achieve the given task. As motor learning is mediated in part by mechanisms of synaptic plasticity (Muellbacher et al., 2002; Sanes & Donoghue, 2000) which underpin the after-effects induced by tDCS (Liebetanz, Nitsche, Tergau, & Paulus, 2002), these behavioral studies support our results which indicate network connectivity is associated with neuroplastic responses following tDCS.

It is perhaps less clear how connectivity in a network approximating the ipsilesional M1, ipsilesional parietal cortex and contralesional frontotemporal region is associated with change in MEP amplitude following tDCS applied to the ipsilesional M1. Although applied to a specific cortical target, it is well established that tDCS generates activity within diffuse brain regions. Both imaging and computational modelling studies have demonstrated that tDCS induced after-effects are widespread and include both cortical and subcortical regions across both hemispheres (Bikson, Rahman, & Datta, 2012; Datta, Truong, Minhas, Parra, & Bikson, 2012; Lang et al., 2005). The magnitude of stimulation effects beyond the target may be related to the degree of connectivity (Cocchi et al., 2015; Hamada et al., 2009). Similarly, imaging studies have demonstrated that TMS applied to M1 activates several cortical regions beyond stimulation site including the contralateral M1 (Bohning et al., 1999, 2000; Hanakawa et al., 2009; Shitara, Shinozaki, Takagishi, Honda, & Hanakawa, 2011). In addition, there is good evidence that manipulation of cortical regions outside M1 can induce measurable changes in MEP amplitude (Buch, Mars, Boorman, & Rushworth, 2010; Duque, Labruna, Verset, Olivier, & Ivry, 2012; Ferbert et al., 1992; Groppa et al., 2012), suggesting circuits which influence the MEP extend beyond M1. The network which generates a MEP must partially overlap with the network activated by tDCS, as MEPs are frequently used to quantify changes in cortical excitability following tDCS. Although difficult to infer generators of neural signals recorded at the scalp with EEG, it may be that stronger connectivity in the reported network allows tDCS to have greater effect on MEP generating circuits.

Functional connectivity in several different frequency bands were investigated, with connectivity in the alpha band providing the strongest association with anodal tDCS response. Previous studies have demonstrated the functional significance of alpha oscillations which have been associated with post stroke subacute clinical status, motor performance and functional recovery (Dubovik et al., 2013; Kawano et al., 2017; Westlake et al., 2012). Furthermore, studies have reported alpha oscillations are associated with attention, memory, motor learning and performance (Harris, Dux, Jones, & Mattingley, 2017; Jensen, Gelfand, Kounios, & Lisman, 2002; Mottaz et al., 2015; Pollok, Boysen, & Krause, 2015). As ischemic lesions result in dysfunction in surviving neural networks, it is unsurprising that alpha oscillations contribute to neuroplastic responses which underpin anodal tDCS. However, strong associations with the anodal tDCS response were also observed for PLS models generated in high beta ($R^2 = 0.59$) and theta ($R^2 = 0.60$) frequency bands. Although individual electrode clusters identified by these PLS models were not significantly associated with anodal tDCS responses, previous studies suggest that high beta and theta band oscillations may have some functional significance with regards to neuroplastic induction. For example, estimates of high beta connectivity have been reported to predict response to tDCS and motor learning in healthy adults (Hordacre et al., 2017b; Wu et al., 2014). Similarly, theta band imaginary coherence, a conservative estimate of connectivity which discards instantaneous interactions to reduce spurious estimates of connectivity, was associated with recovery of language and motor function following stroke (Nicolo et al., 2015). Further work is required to decipher whether network interactions in theta and high beta bands are associated with anodal tDCS response in stroke, however our results clearly show estimates of alpha band functional connectivity provide the strongest marker of neuroplastic induction with the identified electrode clusters consistent across a range of PLS thresholds.

A network approximating the ipsilesional M1, ipsilesional parietal cortex, and contralesional frontotemporal region accounted for a large portion of variance in tDCS response. Although caution is required when suggesting generators of neural signal recorded with EEG surface electrodes, this network may reflect an ipsilesional sensorimotor and contralesional motor–premotor network. The network identified differs to previous studies with healthy adults where ipsilateral sensorimotor network connectivity in the high beta band was associated tDCS response and motor learning (Hordacre et al., 2017b; Wu et al., 2014). The more extensive bilateral network identified in our study with chronic stroke survivors may be explained by previous neuroimaging studies which report movement of the paretic upper limb leads to extensive, bilateral neural activity, not observed in healthy age-matched controls (Grefkes et al., 2008; Ward, Brown, Thompson, & Frackowiak, 2003). This suggests that both hemispheres are functionally integrated to a greater extent during upper limb movement following stroke and may reflect system wide network disturbances (Grefkes & Fink, 2011). The more extensive network activity may also reflect, in-part, differences in topography for alpha and beta oscillations in the sensorimotor system. For example, there is some suggestion that upper limb movement modulates beta activity within the sensorimotor cortex, while alpha activity is widespread and bilateral (McFarland, Miner, Vaughan, & Wolpaw, 2000). However, the PLS model generated in the high beta frequency for this study did indicate that bilateral networks contribute to the anodal tDCS response, and in light of this result, we favor the explanation that bilateral activity reflects neural changes following stroke.

Approaches to facilitate a more efficient or complete functional recovery following stroke are of high value for patients and clinicians. As a result, tDCS and other forms of NIBS hold great promise as an adjuvant or adjunct therapy. However, behavior effects induced by tDCS appear variable (Tedesco Triccas et al., 2016), and it may be that tDCS is most effective in a subset of stroke patients. Robust

biomarkers to predict those likely to benefit would assist clinical translation of this plasticity inducing paradigm. Our results, in a small sample of chronic ischemic stroke survivors, suggest that estimates of alpha band functional connectivity between electrodes approximating an ipsilesional sensorimotor and contralesional motor-premotor network was strongly associated with response to anodal tDCS. This model of connectivity provided a strong predictive capacity (leave one out and predict $R^2 = 0.58$) and appeared to be specific to anodal tDCS, as similar relationships were not observed for sham stimulation. Furthermore, the identified electrode clusters were consistent across a range of PLS thresholds, suggesting that this model of connectivity is robust. Connectivity between the seed electrode and each cluster was also individually associated with anodal tDCS response. Further investigation of connectivity between the seed and ipsilesional parietal cluster revealed a structural measure of impairment (lesion volume) may improve the fit of a regression model accounting for variance in anodal tDCS response; however, this was not observed for the contralesional frontotemporal cluster. The opportunity for both functional measures of connectivity and structural measures of injury to inform anodal tDCS response may help in development of an algorithm to identify patients likely to respond well to tDCS. However, the potential benefit of including structural measures of injury requires further investigation as our evidence only supports a small improvement in model fit. Nevertheless, the current data suggests functional connectivity alone is a robust marker of neuroplastic induction. In support of this finding, baseline functional connectivity, but not MRI measures of lesion volume or corticospinal tract injury, were found to predict improvements in motor function for stroke patients undergoing four weeks of therapy (Wu et al., 2015). These results would appear to infer that functional network measures are more closely associated with stroke neuroplastic response and recovery than structural assessments of injury or patient characteristics. Functional connectivity may have substantial utility as a biomarker to select stroke patients likely to benefit from tDCS. Alternatively, connectivity could be used to provide temporal precision to justify the optimal time to apply tDCS as the motor network is dynamic and undergoes reorganization across acute and subacute phases, both spontaneously and in response to therapy.

Although not reaching statistical significance in this small sample, it is interesting to note that moderate to large effect sizes were observed for a negative correlation between age and both anodal tDCS response and connectivity between electrodes approximating the ipsilesional M1 and parietal cortex. This trend in our data appears to support previous studies indicating greater age is associated with reduced M1 plasticity (Ridding & Ziemann, 2010) and it may be that this is mediated through change in network activity. Similarly, moderate to large effect sizes not reaching statistical significance suggested lesion volume may be positively correlated with both anodal tDCS response and connectivity between electrodes approximating the ipsilesional M1 and contralesional frontotemporal cortex. At first glance it may appear paradoxical that a large lesion would be associated with stronger connectivity between hemispheres. However, this may partially reflect greater reliance on contralesional networks as a result of greater ipsilesional stroke volume. In support, a previous rat study demonstrated larger infarcts were associated with increased recruitment of the contralesional hemisphere following stroke (Biernaskie, Szymanska, Windle, & Corbett, 2005). Similarly, human studies have reported that stroke survivors with larger infarcts demonstrate a shift in activity toward the contralesional hemisphere (Cramer & Crafton, 2006). Together, these results support our observation of increased contralesional network activity in those with larger lesions.

While EEG measures of functional connectivity may be a useful biomarker of neuroplastic induction following tDCS, we acknowledge that EEG suffers from poor spatial resolution and signals recorded at the scalp can be affected by volume conduction (Bastos & Schoffelen, 2016). We have attempted to mitigate these limitations be utilizing a conservative measure of functional connectivity (dwPLI) which biases against interactions where there is a phase difference of 0° or 180°; however, this approach may not completely abolish effects of field spread. Furthermore, when describing our findings we have cautiously referred to electrodes clusters as approximating cortical regions as we do not know where recorded scalp signals are generated. An additional limitation of this study relates to the relatively small and homogeneous sample tested. All participants had a first ever mild to moderate ischemic stroke and were 12–21 months poststroke. Further investigation is required to determine whether these results are relevant for hemorrhagic strokes, patients in the acute or subacute phase, or those with more severe motor impairment. Nevertheless these results provide good evidence to indicate functional connectivity is a strong marker of neuroplastic response to brain stimulation in the tested stroke population.

5 | CONCLUSION

In summary, this study demonstrates that alpha band functional connectivity of an approximate ipsilesional sensorimotor and contralesional motor-premotor network is a robust and specific biomarker of neuroplastic induction following anodal tDCS in chronic stroke survivors. These results contribute to current knowledge around factors which modulate neuroplasticity responses to NIBS and provide further insight to the complex intrinsic characteristics associated with experimental plasticity induction in people with stroke.

ACKNOWLEDGMENTS

BH funded by National Health and Medical Research Council (NHMRC) fellowship (1125054). This was supported by the Sylvia and Charles Viertel Charitable Foundation Clinical Investigator Award (VTL2016CI009).

ORCID

Brenton Hordacre http://orcid.org/0000-0002-7129-6684

REFERENCES

Adeyemo, B. O., Simis, M., Macea, D. D., & Fregni, F. (2012). Systematic review of parameters of stimulation, clinical trial design

characteristics, and motor outcomes in non-invasive brain stimulation in stroke. *Frontiers in Psychiatry*, *3*,

Andersson, C. A., & Bro, R. (2000). The n-way toolbox for MATLAB. *Chemometrics and Intelligent Laboratory Systems*, *52*(1), 1–4.

Banks, J. L., & Marotta, C. A. (2007). Outcomes validity and reliability of the modified rankin scale: Implications for stroke clinical trials. *Stroke*, *38*(3), 1091–1096.

Bastos, A. M., & Schoffelen, J.-M. (2016). A tutorial review of functional connectivity analysis methods and their interpretational pitfalls. *Frontiers in Systems Neuroscience*, *9*,

Biernaskie, J., Szymanska, A., Windle, V., & Corbett, D. (2005). Bi-hemispheric contribution to functional motor recovery of the affected forelimb following focal ischemic brain injury in rats. *European Journal of Neuroscience*, *21*(4), 989–999.

Bikson, M., Rahman, A., & Datta, A. (2012). Computational models of transcranial direct current stimulation. *Clinical EEG and Neuroscience*, *43*(3), 176–183.

Boggio, P. S., Nunes, A., Rigonatti, S. P., Nitsche, M. A., Pascual-Leone, A., & Fregni, F. (2007). Repeated sessions of noninvasive brain dc stimulation is associated with motor function improvement in stroke patients. *Restorative Neurology and Neuroscience*, *25*, 123–129.

Bohning, D., Shastri, A., McConnell, K., Nahas, Z., Lorberbaum, J., Roberts, D., … George, M. (1999). A combined TMS/fMRI study of intensity-dependent TMS over motor cortex. *Biological Psychiatry*, *45*(4), 385–394.

Bohning, D. E., Shastri, A., Wassermann, E. M., Ziemann, U., Lorberbaum, J. P., Nahas, Z., … George, M. S. (2000). Bold-f MRI response to single-pulse transcranial magnetic stimulation (TMS). *Journal of Magnetic Resonance Imaging*, *11*(6), 569–574.

Buch, E. R., Mars, R. B., Boorman, E. D., & Rushworth, M. F. S. (2010). A network centered on ventral premotor cortex exerts both facilitatory and inhibitory control over primary motor cortex during action reprogramming. *Journal of Neuroscience*, *30*(4), 1395–1401.

Cocchi, L., Sale, M. V., Lord, A., Zalesky, A., Breakspear, M., & Mattingley, J. B. (2015). Dissociable effects of local inhibitory and excitatory theta-burst stimulation on large-scale brain dynamics. *Journal of Neurophysiology*, *113*(9), 3375–3385.

Cramer, R. D. (1993). Partial least squares (PLS): Its strengths and limitations. *Perspectives in Drug Discovery and Design*, *1*(2), 269–278.

Cramer, S. C., & Crafton, K. R. (2006). Somatotopy and movement representation sites following cortical stroke. *Experimental Brain Research*, *168*(1–2), 25–32.

Datta, A., Truong, D., Minhas, P., Parra, L. C., & Bikson, M. (2012). Inter-individual variation during transcranial direct current stimulation and normalization of dose using MRI-derived computational models. *Frontiers in Psychiatry*, *3*.

Delorme, A., & Makeig, S. (2004). EEGlab: An open source toolbox for analysis of single-trial EEG dynamics including independent component analysis. *Journal of Neuroscience Methods*, *134*(1), 9–21.

Dubovik, S., Pignat, J. M., Ptak, R., Aboulafia, T., Allet, L., Gillabert, N., … Guggisberg, A. G. (2012). The behavioral significance of coherent resting-state oscillations after stroke. *NeuroImage*, *61*(1), 249–257.

Dubovik, S., Ptak, R., Aboulafia, T., Magnin, C., Gillabert, N., Allet, L., … Guggisberg, A. G. (2013). EEG alpha band synchrony predicts cognitive and motor performance in patients with ischemic stroke. *Behavioural Neurology*, *26*(3), 187–189.

Duque, J., Labruna, L., Verset, S., Olivier, E., & Ivry, R. B. (2012). Dissociating the role of prefrontal and premotor cortices in controlling inhibitory mechanisms during motor preparation. *Journal of Neuroscience*, *32*(3), 806–816.

Elsner, B., Kugler, J., Pohl, M., & Mehrholz, J. (2016). Transcranial direct current stimulation (TDCS) for improving activities of daily living, and physical and cognitive functioning, in people after stroke. *Cochrane Database of Systematic Reviews*, *3*, Cd009645.

Ferbert, A., Priori, A., Rothwell, J. C., Day, B. L., Colebatch, J. G., & Marsden, C. D. (1992). Interhemispheric inhibition of the human motor cortex. *Journal of Physiology*, *453*, 525–546.

Gandiga, P. C., Hummel, F. C., & Cohen, L. G. (2006). Transcranial dc stimulation (TDCS): A tool for double-blind sham-controlled clinical studies in brain stimulation. *Clinical Neurophysiology*, *117*(4), 845–850.

Goldsworthy, M. R., Hordacre, B., & Ridding, M. C. (2016). Minimum number of trials required for within- and between-session reliability of TMS measures of corticospinal excitability. *Neuroscience*, *320*, 205–209.

Grefkes, C., & Fink, G. R. (2011). Reorganization of cerebral networks after stroke: New insights from neuroimaging with connectivity approaches. *Brain*, *134*(Pt 5), 1264–1276.

Grefkes, C., Nowak, D. A., Eickhoff, S. B., Dafotakis, M., Küst, J., Karbe, H., & Fink, G. R. (2008). Cortical connectivity after subcortical stroke assessed with functional magnetic resonance imaging. *Annals of Neurology*, *63*(2), 236–246.

Groppa, S., Schlaak, B. H., Munchau, A., Werner-Petroll, N., Dunnweber, J., Baumer, T., … Siebner, H. R. (2012). The human dorsal premotor cortex facilitates the excitability of ipsilateral primary motor cortex via a short latency cortico-cortical route. *Human Brain Mapping*, *33*(2), 419–430.

Hamada, M., Hanajima, R., Terao, Y., Okabe, S., Nakatani-Enomoto, S., Furubayashi, T., … Ugawa, Y. (2009). Primary motor cortical metaplasticity induced by priming over the supplementary motor area. *Journal of Physiology*, *587*(Pt 20), 4845–4862.

Hamada, M., Murase, N., Hasan, A., Balaratnam, M., & Rothwell, J. C. (2013). The role of interneuron networks in driving human motor cortical plasticity. *Cerebral Cortex (New York, N.Y. : 1991)*, *23*(7), 1593–1605.

Hanakawa, T., Mima, T., Matsumoto, R., Abe, M., Inouchi, M., Urayama, S., … Fukuyama, H. (2009). Stimulus-response profile during single-pulse transcranial magnetic stimulation to the primary motor cortex. *Cerebral Cortex (New York, N.Y. : 1991)*, *19*(11), 2605–2615.

Hao, Z., Wang, D., Zeng, Y., & Liu, M. (2013). Repetitive transcranial magnetic stimulation for improving function after stroke. *Cochrane Database of Systematic Reviews*, *5*, CD008862.

Harris, A. M., Dux, P. E., Jones, C. N., & Mattingley, J. B. (2017). Distinct roles of theta and alpha oscillations in the involuntary capture of goal-directed attention. *NeuroImage*, *152*, 171–183.

He, W., Goodkind, D., & Kowal, P. (2016). An aging world: 2015.

Hesse, S., Waldner, A., Mehrholz, J., Tomelleri, C., Pohl, M., & Werner, C. (2011). Combined transcranial direct current stimulation and robot-assisted arm training in subacute stroke patients. *Neurorehabilitation and Neural Repair*, *25*(9), 838–846.

Hordacre, B., Goldsworthy, M. R., Vallence, A.-M., Darvishi, S., Moezzi, B., Hamada, M., … Ridding, M. C. (2017a). Variability in neural excitability and plasticity induction in the human cortex: A brain stimulation study. *Brain Stimulation*, *10*, 588–595.

Hordacre, B., Moezzi, B., Goldsworthy, M. R., Rogasch, N. C., Graetz, L. J., & Ridding, M. C. (2017b). Resting state functional connectivity measures correlate with the response to anodal transcranial direct current stimulation. *European Journal of Neuroscience*, *45*, 837–845.

Hummel, F., Celnik, P., Giraux, P., Floel, A., Wu, W. H., Gerloff, C., & Cohen, L. G. (2005). Effects of non-invasive cortical stimulation on skilled motor function in chronic stroke. *Brain*, *128*(Pt 3), 490–499.

Jensen, O., Gelfand, J., Kounios, J., & Lisman, J. E. (2002). Oscillations in the alpha band (9–12 hz) increase with memory load during retention in a short-term memory task. *Cerebral Cortex (New York, N.Y. : 1991)*, *12*(8), 877–882.

Kass, R. E., & Raftery, A. E. (1995). Bayes factors. *Journal of the American Statistical Association*, *90*(430), 773–795.

Kawano, T., Hattori, N., Uno, Y., Kitajo, K., Hatakenaka, M., Yagura, H., … Miyai, I. (2017). Large-scale phase synchrony reflects clinical status after stroke: An EEG study. *Neurorehabilitation and Neural Repair*, *31*(6), 561–570.

Khedr, E. M., Ahmed, M. A., Fathy, N., & Rothwell, J. C. (2005). Therapeutic trial of repetitive transcranial magnetic stimulation after acute ischemic stroke. *Neurology*, *65*(3), 466.

Lang, N., Siebner, H. R., Ward, N. S., Lee, L., Nitsche, M. A., Paulus, W., … Frackowiak, R. S. (2005). How does transcranial dc stimulation of the primary motor cortex alter regional neuronal activity in the human brain? *European Journal of Neuroscience*, *22*(2), 495–504.

Liebetanz, D., Nitsche, M. A., Tergau, F., & Paulus, W. (2002). Pharmacological approach to the mechanisms of transcranial dc-stimulation-induced after-effects of human motor cortex excitability. *Brain*, *125* (Pt 10), 2238–2247.

López-Alonso, V., Cheeran, B., Río-Rodríguez, D., & Fernández-del-Olmo, M. (2014). Inter-individual variability in response to non-invasive brain stimulation paradigms. *Brain Stimulation*, *7*(3), 372–380.

McFarland, D. J., Miner, L. A., Vaughan, T. M., & Wolpaw, J. R. (2000). Mu and beta rhythm topographies during motor imagery and actual movements. *Brain Topography*, *12*(3), 177–186.

Menzies, L., Achard, S., Chamberlain, S. R., Fineberg, N., Chen, C. H., del Campo, N., … Bullmore, E. (2007). Neurocognitive endophenotypes of obsessive-compulsive disorder. *Brain*, *130*(Pt 12), 3223–3236.

Mottaz, A., Solcà, M., Magnin, C., Corbet, T., Schnider, A., & Guggisberg, A. G. (2015). Neurofeedback training of alpha-band coherence enhances motor performance. *Clinical Neurophysiology*, *126*(9), 1754–1760.

Muellbacher, W., Ziemann, U., Wissel, J., Dang, N., Kofler, M., Facchini, S., … Hallett, M. (2002). Early consolidation in human primary motor cortex. *Nature*, *415*(6872), 640–644.

Müller-Dahlhaus, J. F., Orekhov, Y., Liu, Y., & Ziemann, U. (2008). Interindividual variability and age-dependency of motor cortical plasticity induced by paired associative stimulation. *Experimental Brain Research*, *187*(3), 467–475.

Murray, C. J., Vos, T., Lozano, R., Naghavi, M., Flaxman, A. D., Michaud, C., … Abdalla, S. (2012). Disability-adjusted life years (dalys) for 291 diseases and injuries in 21 regions, 1990–2010: A systematic analysis for the global burden of disease study 2010. *Lancet*, *380*(9859), 2197–2223.

Nicolo, P., Rizk, S., Magnin, C., Pietro, M. D., Schnider, A., & Guggisberg, A. G. (2015). Coherent neural oscillations predict future motor and language improvement after stroke. *Brain*, *138*(Pt 10), 3048–3060.

Oostenveld, R., Fries, P., Maris, E., & Schoffelen, J.-M. (2011). Fieldtrip: Open source software for advanced analysis of MEG, EEG, and invasive electrophysiological data. *Computational Intelligence and Neuroscience*, *2011*(9), 1.

Park, C-h., Chang, W. H., Ohn, S. H., Kim, S. T., Bang, O. Y., Pascual-Leone, A., & Kim, Y.-H. (2011). Longitudinal changes of resting-state functional connectivity during motor recovery after stroke. *Stroke*, *42* (5), 1357–1362.

Pollok, B., Boysen, A.-C., & Krause, V. (2015). The effect of transcranial alternating current stimulation (TACS) at alpha and beta frequency on motor learning. *Behavioural Brain Research*, *293*, 234–240.

Quinlan, E. B., Dodakian, L., See, J., McKenzie, A., Le, V., Wojnowicz, M., … Cramer, S. C. (2015). Neural function, injury, and stroke subtype predict treatment gains after stroke. *Annals of Neurology*, *77*(1), 132–145.

Ridding, M. C., & Ziemann, U. (2010). Determinants of the induction of cortical plasticity by non-invasive brain stimulation in healthy subjects. *Journal of Physiology*, *588*(13), 2291–2304.

Roger, V. L., Go, A. S., Lloyd-Jones, D. M., Adams, R. J., Berry, J. D., Brown, T. M., … Wylie-Rosett, J. American Heart Association Statistics C, Stroke Statistics S (2011). Heart disease and stroke statistics–2011 update: A report from the American Heart Association. *Circulation*, *123*(4), e18–e209.

Roger, V. L., Go, A. S., Lloyd-Jones, D. M., Benjamin, E. J., Berry, J. D., Borden, W. B., … Fox, C. S. (2012). Heart disease and stroke statistics—2012 update a report from the American Heart Association. *Circulation*, *125*(1), e2–e220.

Rossi, S., Hallett, M., Rossini, P. M., & Pascual-Leone, A. (2011). Screening questionnaire before TMS: An update. *Clinical Neurophysiology*, *122*(8), 1686.

Rossi, C., Sallustio, F., Di Legge, S., Stanzione, P., & Koch, G. (2013). Transcranial direct current stimulation of the affected hemisphere does not accelerate recovery of acute stroke patients. *European Journal of Neurology*, *20*(1), 202–204.

Sanes, J. N., & Donoghue, J. P. (2000). Plasticity and primary motor cortex. *Annual Review of Neuroscience*, *23*, 393–415.

Shitara, H., Shinozaki, T., Takagishi, K., Honda, M., & Hanakawa, T. (2011). Time course and spatial distribution of fMRI signal changes during single-pulse transcranial magnetic stimulation to the primary motor cortex. *NeuroImage*, *56*(3), 1469–1479.

Swayne, O. B. C., Rothwell, J. C., Ward, N. S., & Greenwood, R. J. (2008). Stages of motor output reorganization after hemispheric stroke suggested by longitudinal studies of cortical physiology. *Cerebral Cortex (New York, N.Y. : 1991)*, *18*(8), 1909–1922.

Talelli, P., Greenwood, R. J., & Rothwell, J. C. (2007). Exploring theta burst stimulation as an intervention to improve motor recovery in chronic stroke. *Clinical Neurophysiology*, *118*(2), 333–342.

Tedesco Triccas, L., Burridge, J. H., Hughes, A. M., Pickering, R. M., Desikan, M., Rothwell, J. C., & Verheyden, G. (2016). Multiple sessions of transcranial direct current stimulation and upper extremity rehabilitation in stroke: A review and meta-analysis. *Clinical Neurophysiology*, *127*(1), 946–955.

Tedesco Triccas, L., Burridge, J. H., Hughes, A., Verheyden, G., Desikan, M., & Rothwell, J. (2015). A double-blinded randomised controlled trial exploring the effect of anodal transcranial direct current stimulation and uni-lateral robot therapy for the impaired upper limb in sub-acute and chronic stroke. *NeuroRehabilitation*, *37*(2), 181–191.

Traversa, R., Cicinelli, P., Pasqualetti, P., Filippi, M., & Rossini, P. M. (1998). Follow-up of interhemispheric differences of motor evoked potentials from the 'affected' and 'unaffected' hemispheres in human stroke. *Brain Research*, *803*(1–2), 1–8.

Vinck, M., Oostenveld, R., Van Wingerden, M., Battaglia, F., & Pennartz, C. M. A. (2011). An improved index of phase-synchronization for electrophysiological data in the presence of volume-conduction, noise and sample-size bias. *Neuroimage*, *55*(4), 1548–1565.

Ward, N. S., Brown, M. M., Thompson, A. J., & Frackowiak, R. S. (2003). Neural correlates of motor recovery after stroke: A longitudinal fMRI study. *Brain*, *126*(Pt 11), 2476–2496.

Westerhuis, J. A., de Jong, S., & Smilde, A. K. (2001). Direct orthogonal signal correction. *Chemometrics and Intelligent Laboratory Systems*, *56*(1), 13–25.

Westlake, K. P., Hinkley, L. B., Bucci, M., Guggisberg, A. G., Byl, N., Findlay, A. M., . . . Nagarajan, S. S. (2012). Resting state alpha-band functional connectivity and recovery after stroke. *Experimental Neurology*, *237*(1), 160–169.

Wu, J., Quinlan, E. B., Dodakian, L., McKenzie, A., Kathuria, N., Zhou, R. J., . . . Cramer, S. C. (2015). Connectivity measures are robust biomarkers of cortical function and plasticity after stroke. *Brain*, *138*(Pt 8), 2359–2369.

Wu, J., Srinivasan, R., Kaur, A., & Cramer, S. C. (2014). Resting-state cortical connectivity predicts motor skill acquisition. *NeuroImage*, *91*, 84–90.

Yach, D., Hawkes, C., Gould, C. L., & Hofman, K. J. (2004). The global burden of chronic diseases: Overcoming impediments to prevention and control. *JAMA*, *291*(21), 2616–2622.

How to cite this article: Hordacre B, Moezzi B, Ridding MC. Neuroplasticity and network connectivity of the motor cortex following stroke: A transcranial direct current stimulation study. *Hum Brain Mapp*. 2018;39:3326–3339. https://doi.org/10.1002/hbm.24079